Atmos. Chem. Phys. Discuss., doi:10.5194/acp-2016-392, 2016
Manuscript under review for journal Atmos. Chem. Phys.
Published: 3 June 2016

Atmospheric Chemistry and Physics Discussions

First detection of ammonia (NH_3) in the Asian monsoon upper troposphere

Michael Höpfner[1], Rainer Volkamer[2,3], Udo Grabowski[1], Michel Grutter[4], Johannes Orphal[1], Gabriele Stiller[1], Thomas von Clarmann[1], and Gerald Wetzel[1]

[1]Institute of Meteorology and Climate Research, Karlsruhe Institute of Technology, Karlsruhe, Germany.
[2]Department of Chemistry & Biochemistry, University of Colorado, Boulder, CO, USA.
[3]Cooperative Institute for Research in Environmental Sciences, University of Colorado at Boulder, CO, USA.
[4]Centro de Ciencias de la Atmósfera, Universidad Nacional Autónoma de México, Mexico City, Mexico.

Correspondence to: M. Höpfner (michael.hoepfner@kit.edu)

Abstract. Ammonia (NH_3) has been detected in the upper troposphere by analysis of averaged MIPAS (Michelson Interferomter for Passive Atmospheric Sounding) infrared limb-emission spectra. We have found enhanced amounts of NH_3 within the region of the Asian monsoon at 12–15 km altitude. Three-monthly, 10° longitude × 10° latitude average profiles reaching maximum mixing ratios of around 30 $pptv$ in this altitude range have been retrieved with a vertical resolution of 3–8 km and estimated errors of about 5 $pptv$. These observations show that loss processes during transport from the boundary layer to the upper troposphere within the Asian monsoon do not deplete the air entirely of NH_3. Thus, ammonia might contribute to the so-called Asian tropopause aersol layer by formation of ammonium aerosol particles. On a global scale, outside the monsoon area and during different seasons, we could not detect enhanced values of NH_3 above the actual detection limit of about 3-5 $pptv$. This upper bound helps to constrain global model simulations.

1 Introduction

In the Earth's atmosphere the trace gas ammonia (NH_3) represents the major form of reduced nitrogen. With a share of around 70–80%, the wealth of ammonia emissions is due to anthropogenic activity, namely by use of synthetic fertilizers and livestock manure management (Bouwman et al., 1997; Paulot et al., 2015). Major source regions of NH_3 are located in south-east China and, northern India (Paulot et al., 2014; Van Damme et al., 2015).

Neutralization of acids by the alkaline gas NH_3 leads to the formation of ammonium salts in the atmosphere. For example, reaction of NH_3 with sulfuric acid (H_2SO_4) or nitric acid (HNO_3) forms aerosol particles composed of ammonium sulfate, $(NH_4)_2SO_4$ or ammonium nitrate, NH_4NO_3 (e.g. Behera et al., 2013, and references therein). These inorganic aerosols are important not only with re-

Atmos. Chem. Phys. Discuss., doi:10.5194/acp-2016-392, 2016
Manuscript under review for journal Atmos. Chem. Phys.
Published: 3 June 2016

Atmospheric Chemistry and Physics Discussions

gard to air quality considerations (Hamaoui-Laguel et al., 2014) but they also affect climate through various direct and indirect radiative impacts (Adams et al., 2001; Martin et al., 2004; Liao and Seinfeld, 2005; Forster et al., 2007; Xu and Penner, 2012; Boucher et al., 2013). Further, also cirrus clouds might be affected by the presence of NH_3 and ammonium (Tabazadeh and Toon, 1998; Wang et al., 2008). E.g. ammonium sulfate aerosols that are partially coated and have exposed surface sites are active with respect of ice nucleation (Prenni et al., 2001; Wise et al., 2004). Moreover, through stabilization of sulfuric acid clusters, ammonia itself may play an important role regarding the initial nucleation of sulfuric acid aerosols (Ortega et al., 2008; Kirkby et al., 2011; Schobesberger et al., 2013; Kürten et al., 2015).

Global emissions of NH_3 are expected to rise strongly due to the need to sustain a growing population and due to enhanced emissions under increasing temperatures (Erisman et al., 2008; Vuuren et al., 2011; Sutton et al., 2013). As a result, in future prospects a positive radiative forcing by a decrease of the shortwave albedo caused by reductions of industrial SO_2 emissions may partly be compensated by increasing amounts of ammonium containing aerosols (Bellouin et al., 2011; Xu and Penner, 2012; Shindell et al., 2013; Hauglustaine et al., 2014).

Before 2008, measurements of ammonia were almost exclusively based on in-situ technologies (von Bobrutzki et al., 2010). A first step in the direction of observations with global coverage was achieved by Beer et al. (2008) who reported the detection of NH_3 in the lower troposphere from space-borne nadir sounding measurements by the Tropospheric Emission Spectrometer (TES) on the EOS Aura satellite. Subsequently, various papers have been published describing retrieval, validation and interpretation of NH_3 derived from the nadir sounders TES (Clarisse et al., 2010; Shephard et al., 2011), IASI (Infrared Atmospheric Sounding Interferometer) (Coheur et al., 2009; Clarisse et al., 2009, 2010; Van Damme et al., 2014), CrIS (Cross-track Infrared Sounder) (Shephard and Cady-Pereira, 2015), and AIRS (Atmospheric Infrared Sounder) (Warner et al., 2016). Recently, retrievals of NH_3 vertical column amounts from ground-based FTIR solar observations located at various sites have been presented by Dammers et al. (2015) and are being used for the quantitative validation of space-borne nadir-viewing datasets (Dammers et al., 2016).

All these observations sample atmospheric NH_3 either as in-situ concentrations on ground or from ground or space as total column amounts, which are dominated by the large amounts in the lower part of the atmosphere. With regard to the predicted increase in NH_3 emissions and the possible compensating effect on aerosol radiative forcing, Paulot et al. (2016) emphasize the need to better constrain also the vertical distribution of ammonia. However, there is a vast lack of observations of NH_3 at mid- and upper tropospheric levels.

Vertical profiles of NH_3 concentrations through airborne in-situ observations are very sparse, reaching maximum altitudes of about 5.5 km (Nowak et al., 2010; Leen et al., 2013) with detection limits for NH_3 of 70 pptv and maximum observed values at 4–5.5 km of 300–500 pptv (Nowak et al., 2010).

Atmos. Chem. Phys. Discuss., doi:10.5194/acp-2016-392, 2016
Manuscript under review for journal Atmos. Chem. Phys.
Published: 3 June 2016

Atmospheric Chemistry and Physics Discussions

At higher altitudes, Oelhaf et al. (1983) reported upper limits of 100 pptv above 10 km by analysis of balloon-borne limb-transmission spectra. In-situ observations by Ziereis and Arnold (1986) restricted the concentrations to below the pptv-range between 8 and 10 km.

In case of space-borne limb sounding instruments no unequivocal detection of NH_3 has been published so far. Burgess et al. (2006) report on first attempts to retrieve ammonia distributions from the Michelson Interferometer for Passive Atmospheric Sounding (MIPAS) on Envisat but no spectral evidence for its presence is presented. Further, within a plume of biomass burning observed with the ACE-FTS instrument, Coheur et al. (2007) mention only a "tentative identification" of NH_3 while the spectral signals of various other trace species, like C_2H_4, C_3H_6O, H_2CO and PAN were detected unequivocally.

In the work presented below we show the first evidence for the presence of NH_3 together with quantitative retrievals at upper tropospheric levels by use of MIPAS averaged limb spectra.

2 MIPAS/Envisat

On board the Envisat satellite the MIPAS limb sounder recorded infrared spectra of the radiation emitted by atmospheric constituents from June 2002 until April 2012 (Fischer et al., 2008). Between June 2002 and March 2004 (period 1) the spectral resolution was 0.025 cm^{-1} with one limb-scan consisting of 17 spectra from about 6–60 km altitude with steps of 3 km in the UTLS in case of nominal mode observations. From January 2005 until April 2012 (period 2) the spectral resolution was degraded to 0.0625 cm^{-1}. This was accompanied by a better vertical sampling (27 tangent levels with 1.5 km steps in the UTLS). Also in horizontal direction along the satellite track the sampling improved from a distance between subsequent limb-scans of 550 km during period 1 to 420 km during period 2.

3 Retrieval and spectral detection

Here we report on the detection and retrieval of NH_3 from MIPAS observations in the upper troposphere on basis of averaged limb-spectra. This method has already been applied successfully for the detection of bromine nitrate ($BrONO_2$) (Höpfner et al., 2009) and for the compilation of a global climatology of stratospheric sulfur dioxide (SO_2) from MIPAS measurements (Höpfner et al., 2013). In these investigations the mean spectra consisted of monthly zonal averages within 10° latitude intervals whereas for the present work we have chosen seasonal (3-monthly) averages within bins of 10° latitude by 10° longitude. Thus, we have refrained from zonal averaging in order to obtain resolution in meridional direction albeit slightly sacrificing temporal resolution. To obtain at least a reduction of the spectral noise of at least a factor of five, we have chosen a lower limit of 25 single spectra (MIPAS level-1b version 5) for averaging. In the troposphere the number of available spectra is limited as a result of cloud contamination along the limb line-of-sight. We have applied a

Atmos. Chem. Phys. Discuss., doi:10.5194/acp-2016-392, 2016
Manuscript under review for journal Atmos. Chem. Phys.
Published: 3 June 2016

Atmospheric Chemistry and Physics Discussions

cloud filter to deselect cloud-contaminated spectra before averaging. As cloud detection scheme the established cloud-index method (Spang et al., 2004) with a cloud index limit of 2.0 has been used.

To derive altitude profiles of NH_3 from each averaged limb-scan we have applied a constrained non-linear multi-parameter least-squares fitting procedure where measurements from all spectra of one limb scan are analysed in one step (e.g., von Clarmann et al., 2003; Höpfner et al., 2009). The unknown atmospheric state is described in terms of trace gas volume mixing ratios at discrete altitude levels with a grid distance of 1 km within the region of the UTLS. This grid is finer compared to the instrumental vertical field-of-view width of about 3 km at the tangent points and also finer than the vertical sampling distance of 1.5–3 km. To dampen vertical oscillations arising from the ill-posedness of the inverse problem a first oder smoothing constraint has been chosen (Tikhonov, 1963; Steck, 2002). The regularization strengths have been adjusted independently for each species being retrieved simultaneously.

For fitting of the NH_3 signatures we have chosen spectral windows within the interval 950–970 cm^{-1} which have the advantage that they are situated in the region of one of the optically thinnest mid-infrared atmospheric windows. Furthermore, there are relatively few spectrally interfering species which have to be retrieved simultaneously to NH_3. Spectroscopic line parameters of the HITRAN 2012 database (Rothman et al., 2013) have been used.

A scheme consisting of two subsequent steps has been identified as adequate for the retrieval of NH_3. First, the broader wavenumber range 962–968 cm^{-1} has been chosen to fit the strong CO_2 lines of the laser band together with the interfering species O_3, H_2O, NH_3, COF_2. In the second step, narrow analysis windows have been placed around the strongest signatures of NH_3: 951.6–952.0 cm^{-1}, 965.1–965.6 cm^{-1}, and 966.6–967.5 cm^{-1} (MIPAS period 1) and 951.625–952.0 cm^{-1}, 965.125–965.625 cm^{-1}, and 966.625–967.5 cm^{-1} (MIPAS period 2), thereby avoiding the peaks of the strong CO_2 lines. At this stage CO_2 is kept fixed to the results from the initial retrieval while O_3, H_2O and COF_2 are retrieved jointly with NH_3.

Figure 1 presents the spectral fit and the detection of NH_3 for two examples from both MIPAS periods at tangent heights around 12.5 km within the region of the Asian monsoon in June-August 2003 (top panel) and 2009 (bottom panel). Within each panel the top row shows the observations in black, the fit without taking NH_3 into account in blue and the retrieval including NH_3 in red. In the second row of each panel the residual spectra are shown for the retrieval without (blue) and with (red) consideration of NH_3. Here the green line is the difference between both simulations (with minus without NH_3) in order to show the spectral signature of NH_3 without any instrumental effect, like spectral noise.

The top panel of Fig. 1 reveals clearly the presence of NH_3 in MIPAS limb spectra. Radiative transfer simulations without consideration of NH_3 lead to largest residuals at the position of the ammonia lines. Only when ammonia is taken into account, the observed spectra within all three microwindows are fitted sufficiently well. Comparing the first row of the bottom panel in Fig. 1

Atmos. Chem. Phys. Discuss., doi:10.5194/acp-2016-392, 2016
Manuscript under review for journal Atmos. Chem. Phys.
Published: 3 June 2016

Atmospheric Chemistry and Physics Discussions

with that of the top panel, the worse spectral resolution of MIPAS period 2 becomes obvious. Still the residuals of the NH_3 spectral lines and the better fit upon their consideration are visible, especially in microwindows 2 and 3.

Results of the altitude dependent error estimation are presented in Fig. 2 for the two examples of the limb scans for which the spectral fits have been shown in Fig. 1. A summary of the assumptions on the various sources of uncertainty is provided in Table 1. For spectral noise, the actual error numbers referring to the two limb-scans discussed are given together with their range over all observations in brackets. While noise is directly mapped into the state space for each individual retrieval, the error estimation for all other uncertainties has been performed by sensitivity calculations for atmospheric conditions representative for observations within the influence of the Asian monsoon (Höpfner et al., 2009; Höpfner et al., 2013).

In the left panels of Fig. 2 the bold dotted curves indicate the reconstructed vertical profiles of NH_3. The concentrations reach maximum values of around 24–29 pptv. The bold solid lines represent the total error calculated as the square root of the sum of all error components. The total errors amount to around 2–6 pptv (17–80%) in the altitude region up to about 20 km. Above, the estimated errors are larger than the mixing ratios of NH_3. The leading error components are tangent altitude uncertainties, uncertainties in the HITRAN line intensity data of NH_3 and nonlinearity effects in the averaging procedure as discussed in Höpfner et al. (2009). On the other hand, the use of averaged spectra reduces the noise term to less than 1 pptv within the altitude range of interest.

The vertical resolution of the resulting altitude profiles of NH_3 mixing ratios is directly connected to the noise error values through the applied setting of the regularization strength. The altitude resolution of the retrieval is described by the retrieval averaging kernel matrix (Rodgers, 2000). Examples for both MIPAS periods are provided in Fig. 3. From these, typical vertical resolutions are derived as the retrieval grid width divided by the inverse of the diagonal matrix elements (Rodgers, 2000). Within the altitude region up to 20 km the resulting vertical resolutions vary between 4–8 km during period 1 and 3–6 km during period 2.

4 The global dataset

Retrievals of NH_3 have been performed for the entire period of MIPAS observations, i.e. from July 2002 until April 2012. Figure 4 presents the global volume mixing ratio distributions at 15 km altitude during seven seasons from July 2002 until February 2004. There are enhanced values of up to 33 pptv within a region between 30°–110°E and 20°–50°N during boreal summer, coinciding with the occurrence of the Asian monsoons. During all other seasons and outside the region influenced by the Asian monsoon, no similarly high concentrations of NH_3 can be found.

An overview for all years with sufficient data coverage in the Asian summer monsoon season during the MIPAS mission lifetime is provided in Fig. 5 for altitude levels of 12, 15, and 18 km. Due

Atmos. Chem. Phys. Discuss., doi:10.5194/acp-2016-392, 2016
Manuscript under review for journal Atmos. Chem. Phys.
Published: 3 June 2016

Atmospheric Chemistry and Physics Discussions

to the less frequent presence of clouds, the number of pixels with valid measurements increases with altitude. Similar to the results from MIPAS period 1, also during period 2 the enhancement of NH_3 within the Asian monsoon region is present for all years of observation. Further, on a global scale there are no other areas visible in the dataset with similarly enhanced values of NH_3. While at 12 and 15 km altitude NH_3 enhancements compared to the global background state are visible during all years, at 18 km altitude increased values of NH_3 are present only during the years 2003, 2008, and 2010.

A comparison between vertical profiles of NH_3 averaged within the western (30–70°E, solid lines) and eastern (70–110°E, dashed lines) part of the monsoon region for the latitude band 30–40°N is presented in Fig. 6 for the years 2003 and 2007–2011. In the same Figure, the dotted curve shows the NH_3 mean profile of all years outside the Asian monsoon area, for the same longitude and latitude range (30–110°E, 30–40°S) of the southern hemisphere. The profiles in the region of the Asian monsoon reveal that the maximum concentrations of NH_3 are always larger within the eastern part of the Asian monsoon, reaching values of 10–22 pptv at 11-13 km altitude. Largest vmr values are found in 2003 and 2009 and lowest ones in 2007 and 2011.

In the western part of the area influenced by the Asian monsoon, enhanced averaged volume mixing ratios of NH_3 can only be observed during the years 2003, 2008, and 2010 with values ranging from 6 to 15 pptv. Situated at around 13–15 km, the maximum concentrations in the western part are located always at higher altitudes compared to those from the eastern part of the monsoon region.

The mean NH_3 profiles of the western part show no clear enhancements during the years 2007, 2009 and 2011. These profiles exhibit maximum values below 5 pptv which are in the range of concentrations retrieved in case of the 'background' state of the southern hemisphere (indicated as dotted lines in Fig. 6). These values are below our estimated detection limit (see below).

5 Discussion

As mentioned in the introduction, observations of NH_3 reaching upper tropospheric levels have been published by Ziereis and Arnold (1986). They report upper limits of about 0.04 pptv between 8 and 10 km over Germany in May 1985. At the present state of our MIPAS data analysis we cannot contradict those upper values outside the influence of the Asian monsoon system. Given the total error of a few pptv we would estimate the 1-σ detection limit of our retrieval to be about 3–5 pptv. One might argue that the use of a 1-σ detection limit does not provide sufficiently significant evidence of the NH_3 enhancement within the monsoon. However, random errors cannot explain why the enhancements should appear in a contiguous geographical pattern. Further, the detected enhancements are in many cases well above the 15 pptv and, thus, larger than a 3-σ limit.

Atmos. Chem. Phys. Discuss., doi:10.5194/acp-2016-392, 2016
Manuscript under review for journal Atmos. Chem. Phys.
Published: 3 June 2016

Atmospheric Chemistry and Physics Discussions

Regarding the retrievals outside the monsoon area, there is a difference between the two MIPAS measurement periods at 10–12 km altitude (see e.g. the difference in the dotted lines in Fig. 6 or the higher background level at 12 km altitude visible in Fig. 5 between the year 2003 and 2007–2011) which amounts up to 4 pptv. We attribute this discrepancy to an unexplained systematic uncertainty caused by the different spectral resolutions between both instrumental states. This observation corroborates our error estimation and supports our conclusion that retrieved values up to 3–5 pptv are below the detection limit of the actual dataset.

Nonetheless, our measurements impose constraints on the global distribution of upper tropospheric NH_3 concentrations which can be compared to results from model calculations. One of the first globally modeled distributions of NH_3 has been presented by Dentener and Crutzen (1994, their Fig. 2b). Yearly mean mixing ratios of below 2 pptv are modeled at upper tropospheric levels at mid- and high-latitudes. These are in agreement with the MIPAS background values. However, at equatorial and sub-tropical latitudes, annual mean values of some tens of pptv were simulated between 300 hPa and 200 hPa which are clearly larger than the MIPAS results. Dentener and Crutzen (1994) attributed these values to natural emissions in the tropics. The comparison with our results indicates that either these emissions might have been over- or the tropical sink processes of NH_3 underestimated. In their conclusions Dentener and Crutzen (1994) also mention high modeled concentrations of NH_3 in the free troposphere over India and China. However, since these enhancements were not quantified, they cannot be compared to our observations.

In contrast to Dentener and Crutzen (1994), the zonal and yearly averages of modeled NH_3 shown in Feng and Penner (2007, Fig. 9) decrease to well below 10 pptv above 500 hPa also in tropical regions. Thus, these are more compatible with the MIPAS dataset.

Globally resolved annual mean model results of NH_3 are given in Adams et al. (1999, Plate 3a). Mean mixing ratios of about 3.2 pptv at the 200 hPa pressure level are reported. At that pressure level, a slight gradient between both hemispheres is visible with values of 0–1 pptv in the south and 3–10 pptv in the north. We do not recognize such a gradient in the background NH_3 concentrations from the MIPAS measurements, albeit, compared to our estimated error, we cannot clearly refute such a gradient.

Regarding ammonium nitrate aerosol during the Asian monsoon season, Metzger et al. (2002) discuss their model results of enhanced values at upper tropospheric levels over Asia. These high amounts of ammonium nitrate are attributed to in-situ production from NH_3 (and HNO_3) being convectively transported to upper tropospheric levels. The fact that NH_3 is not removed by dissolution in droplets and subsequent rainout is explained by the low acidity of convective clouds by which only part of the NH_3 would be dissolved. Our observations support these results with respect to the enhanced amounts of NH_3 which obviously survive the uplift within the Asian monsoon circulation. This indicates that a part of the Asian tropopause aerosol layer (ATAL) (Vernier et al., 2011) might be composed of ammonium nitrate, ammonium sulfate or other ammonium containing particles.

Atmos. Chem. Phys. Discuss., doi:10.5194/acp-2016-392, 2016
Manuscript under review for journal Atmos. Chem. Phys.
Published: 3 June 2016

Atmospheric Chemistry and Physics Discussions

Further, through a possible influence of the Asian monsoon on the composition of the tropical tropopause layer (TTL), by transport of ammonia or ammonium our measurements may help to explain why in-situ measurements of aerosols in the TTL indicate that the sulfate is nearly or fully neutralized (Froyd et al., 2009, 2010).

6 Conclusions

We have presented first evidence for ammonia being present in the Earth's upper troposphere by analysis of MIPAS infrared limb emission spectra. The region and period of detection is confined to the Asian monsoon system. Maximum average values of around 30 pptv over a three-monthly period have been retrieved, thus, demonstrating that part of the NH_3 released on ground survives the loss processes on its way to the upper troposphere. As suggested by Metzger et al. (2002), ammonia may form ammonium nitrate aerosols under those circumstances. Thus, our observations indicate a possible contribution of ammonium aerosols to the composition of the ATAL.

The detection of enhanced amounts of NH_3 in the Western part of the Asian monsoon anticyclone during several years suggests that its lifetime is long enough to survive transport far from the source region. The position of the NH_3 maximum at higher altitudes in the Western compared to the Eastern part of the monsoon system is compatible with the general view: mainly convective uplift of boundary layer air in the East followed by upper tropospheric transport and further uplift in the anticyclone towards the West. The generally lower mixing ratios of NH_3 in the Western compared to the Eastern part indicate on-going loss processes at high altitudes.

Unfortunately, in the literature there seem to exist no locally resolved model results of NH_3 during the monsoon period to which we could compare our observations. We anticipate that such simulations would be of value to improve our understanding of NH_3 loss processes and aerosol production in the Asian monsoon. Also, airborne remote sensing observations like the one planned within the EU project StratoClim with the GLORIA instrument on the Geophysica high flying aircraft, will strongly increase our knowledge about ammonia distributions in the Asian monsoon on a much finer time-, horizontal and vertical resolution scale than the MIPAS dataset presented here.

Regarding the global distribution of upper tropospheric NH_3 outside the Asian monsoon, within this study we could provide upper limits in the range of a few pptv. This will help to constrain global models and to improve their results.

Acknowledgements. We acknowledge provision of MIPAS level-1b calibrated spectra by ESA and meteorological analysis data by ECMWF. The research leading to these results has received funding from the European Community's Seventh Framework Programme (FP7/2007-2013) under grant agreement 603557. R.V. is recipient of a KIT Distinguished Intl Scholar award, and acknowledges funding from the U.S. National Science Foundation EAGER award AGS-1452317. We acknowledge support by the Deutsche Forschungsgemeinschaft and Open Access Publishing Fund of the Karlsruhe Institute of Technology.

Atmos. Chem. Phys. Discuss., doi:10.5194/acp-2016-392, 2016
Manuscript under review for journal Atmos. Chem. Phys.
Published: 3 June 2016

Atmospheric Chemistry and Physics Discussions

References

Adams, P. J., Seinfeld, J. H., and Koch, D. M.: Global concentrations of tropospheric sulfate, nitrate, and ammonium aerosol simulated in a general circulation model, J. Geophys. Res., 104, 13 791–13 823, doi:10.1029/1999JD900083, http://dx.doi.org/10.1029/1999JD900083, 1999.

Adams, P. J., Seinfeld, J. H., Koch, D., Mickley, L., and Jacob, D.: General circulation model assessment of direct radiative forcing by the sulfate-nitrate-ammonium-water inorganic aerosol system, J. Geophys. Res., 106, 1097–1111, doi:10.1029/2000JD900512, http://dx.doi.org/10.1029/2000JD900512, 2001.

Beer, R., Shephard, M. W., Kulawik, S. S., Clough, S. A., Eldering, A., Bowman, K. W., Sander, S. P., Fisher, B. M., Payne, V. H., Luo, M., Osterman, G. B., and Worden, J. R.: First satellite observations of lower tropospheric ammonia and methanol, Geophys. Res. Lett., 35, n/a–n/a, doi:10.1029/2008GL033642, http://dx.doi.org/10.1029/2008GL033642, 2008.

Behera, S. N., Sharma, M., Aneja, V. P., and Balasubramanian, R.: Ammonia in the atmosphere: a review on emission sources, atmospheric chemistry and deposition on terrestrial bodies, Environmental Science and Pollution Research, 20, 8092–8131, doi:10.1007/s11356-013-2051-9, http://dx.doi.org/10.1007/s11356-013-2051-9, 2013.

Bellouin, N., Rae, J., Jones, A., Johnson, C., Haywood, J., and Boucher, O.: Aerosol forcing in the Climate Model Intercomparison Project (CMIP5) simulations by HadGEM2-ES and the role of ammonium nitrate, J. Geophys. Res., 116, n/a–n/a, doi:10.1029/2011JD016074, http://dx.doi.org/10.1029/2011JD016074, d20206, 2011.

Boucher, O., Randall, D., Artaxo, P., Bretherton, C., Feingold, G., Forster, P., Kerminen, V.-M., Kondo, Y., Liao, H., Lohmann, U., Rasch, P., Satheesh, S., Sherwood, S., Stevens, B., and Zhang, X.: Clouds and Aerosols, Cambridge University Press, Cambridge, United Kingdom and New York, NY, USA, 2013.

Bouwman, A., Lee, D., Asman, W., Dentener, F., Van Der Hoek, K., and Olivier, J.: A global high-resolution emission inventory for ammonia, Global biogeochemical cycles, 11, 561–587, 1997.

Burgess, A., Dudhia, A., Grainger, R., and Stevenson, D.: Progress in tropospheric ammonia retrieval from the {MIPAS} satellite instrument, Adv. Space Res., 37, 2218 – 2221, doi:http://dx.doi.org/10.1016/j.asr.2005.06.073, http://www.sciencedirect.com/science/article/pii/S0273117705008367, 2006.

Clarisse, L., Clerbaux, C., Dentener, F., Hurtmans, D., and Coheur, P.-F.: Global ammonia distribution derived from infrared satellite observations, Nature Geosci., 2, 479–483, doi:10.1038/ngeo551, http://dx.doi.org/10.1038/ngeo551, 2009.

Clarisse, L., Shephard, M. W., Dentener, F., Hurtmans, D., Cady-Pereira, K., Karagulian, F., Van Damme, M., Clerbaux, C., and Coheur, P.-F.: Satellite monitoring of ammonia: A case study of the San Joaquin Valley, J. Geophys. Res., 115, n/a–n/a, doi:10.1029/2009JD013291, http://dx.doi.org/10.1029/2009JD013291, d13302, 2010.

Coheur, P.-F., Herbin, H., Clerbaux, C., Hurtmans, D., Wespes, C., Carleer, M., Turquety, S., Rinsland, C. P., Remedios, J., Hauglustaine, D., Boone, C. D., and Bernath, P. F.: ACE-FTS observation of a young biomass burning plume: first reported measurements of C_2H_4, C_3H_6O, H_2CO and PAN by infrared occultation from space, Atmos. Chem. Phys., 7, 5437–5446, doi:10.5194/acp-7-5437-2007, http://www.atmos-chem-phys.net/7/5437/2007/, 2007.

Atmos. Chem. Phys. Discuss., doi:10.5194/acp-2016-392, 2016
Manuscript under review for journal Atmos. Chem. Phys.
Published: 3 June 2016

Coheur, P.-F., Clarisse, L., Turquety, S., Hurtmans, D., and Clerbaux, C.: IASI measurements of reactive trace species in biomass burning plumes, Atmos. Chem. Phys., 9, 5655–5667, doi:10.5194/acp-9-5655-2009, http://www.atmos-chem-phys.net/9/5655/2009/, 2009.

Dammers, E., Vigouroux, C., Palm, M., Mahieu, E., Warneke, T., Smale, D., Langerock, B., Franco, B., Van Damme, M., Schaap, M., Notholt, J., and Erisman, J. W.: Retrieval of ammonia from ground-based FTIR solar spectra, Atmos. Chem. Phys., 15, 12 789–12 803, doi:10.5194/acp-15-12789-2015, http://www.atmos-chem-phys.net/15/12789/2015/, 2015.

Dammers, E., Palm, M., Van Damme, M., Vigouroux, C., Smale, D., Conway, S., Toon, G. C., Jones, N., Nussbaumer, E., Warneke, T., Petri, C., Clarisse, L., Clerbaux, C., Hermans, C., Lutsch, E., Strong, K., Hannigan, J. W., Nakajima, H., Morino, I., Herrera, B., Stremme, W., Grutter, M., Schaap, M., Wichink Kruit, R. J., Notholt, J., Coheur, P.-F., and Erisman, J. W.: An evaluation of IASI-NH3 with ground-based FTIR measurements, Atmospheric Chemistry and Physics Discussions, 2016, 1–30, doi:10.5194/acp-2016-141, http://www.atmos-chem-phys-discuss.net/acp-2016-141/, 2016.

Dentener, F. J. and Crutzen, P. J.: A three-dimensional model of the global ammonia cycle, Journal of Atmospheric Chemistry, 19, 331–369, doi:10.1007/BF00694492, http://dx.doi.org/10.1007/BF00694492, 1994.

Erisman, J. W., Sutton, M. A., Galloway, J., Klimont, Z., and Winiwarter, W.: How a century of ammonia synthesis changed the world, Nature Geosci., 1, 636–639, doi:10.1038/ngeo325, 2008.

Feng, Y. and Penner, J. E.: Global modeling of nitrate and ammonium: Interaction of aerosols and tropospheric chemistry, J. Geophys. Res., 112, n/a–n/a, doi:10.1029/2005JD006404, http://dx.doi.org/10.1029/2005JD006404, d01304, 2007.

Fischer, H., Birk, M., Blom, C., Carli, B., Carlotti, M., von Clarmann, T., Delbouille, L., Dudhia, A., Ehhalt, D., Endemann, M., Flaud, J. M., Gessner, R., Kleinert, A., Koopman, R., Langen, J., López-Puertas, M., Mosner, P., Nett, H., Oelhaf, H., Perron, G., Remedios, J., Ridolfi, M., Stiller, G., and Zander, R.: MIPAS: an instrument for atmospheric and climate research, Atmos. Chem. Phys., 8, 2151–2188, 2008.

Forster, P., Ramaswamy, V., Artaxo, P., Berntsen, T., Betts, R., Fahey, D., Haywood, J., Lean, J., Lowe, D., Myhre, G., Nganga, J., Prinn, R., Raga, G., Schulz, M., and Van Dorland, R.: Changes in Atmospheric Constituents and in Radiative Forcing, pp. 129–243, Cambridge University Press, Cambridge, United Kingdom and New York, NY, USA, 2007.

Froyd, K. D., Murphy, D. M., Sanford, T. J., Thomson, D. S., Wilson, J. C., Pfister, L., and Lait, L.: Aerosol composition of the tropical upper troposphere, Atmospheric Chemistry and Physics, 9, 4363–4385, doi:10.5194/acp-9-4363-2009, http://www.atmos-chem-phys.net/9/4363/2009/, 2009.

Froyd, K. D., Murphy, D. M., Lawson, P., Baumgardner, D., and Herman, R. L.: Aerosols that form subvisible cirrus at the tropical tropopause, Atmospheric Chemistry and Physics, 10, 209–218, doi:10.5194/acp-10-209-2010, http://www.atmos-chem-phys.net/10/209/2010/, 2010.

Hamaoui-Laguel, L., Meleux, F., Beekmann, M., Bessagnet, B., Génermont, S., Cellier, P., and Létinois, L.: Improving ammonia emissions in air quality modelling for France, Atmospheric Environment, 92, 584 – 595, doi:http://dx.doi.org/10.1016/j.atmosenv.2012.08.002, http://www.sciencedirect.com/science/article/pii/S1352231012007662, 2014.

Atmos. Chem. Phys. Discuss., doi:10.5194/acp-2016-392, 2016
Manuscript under review for journal Atmos. Chem. Phys.
Published: 3 June 2016

Atmospheric Chemistry and Physics Discussions

Hauglustaine, D. A., Balkanski, Y., and Schulz, M.: A global model simulation of present and future nitrate aerosols and their direct radiative forcing of climate, Atmos. Chem. Phys., 14, 11 031–11 063, doi:10.5194/acp-14-11031-2014, http://www.atmos-chem-phys.net/14/11031/2014/, 2014.

Höpfner, M., von Clarmann, T., Fischer, H., Funke, B., Glatthor, N., Grabowski, U., Kellmann, S., Kiefer, M., Linden, A., Milz, M., Steck, T., Stiller, G. P., Bernath, P., Blom, C. E., Blumenstock, T., Boone, C., Chance, K., Coffey, M. T., Friedl-Vallon, F., Griffith, D., Hannigan, J. W., Hase, F., Jones, N., Jucks, K. W., Keim, C., Kleinert, A., Kouker, W., Liu, G. Y., Mahieu, E., Mellqvist, J., Mikuteit, S., Notholt, J., Oelhaf, H., Piesch, C., Reddmann, T., Ruhnke, R., Schneider, M., Strandberg, A., Toon, G., Walker, K. A., Warneke, T., Wetzel, H., Wood, S., and Zander, R.: Validation of MIPAS $ClONO_2$ measurements, Atmos. Chem. Phys., 7, 257–281, 2007.

Höpfner, M., Orphal, J., von Clarmann, T., Stiller, G., and Fischer, H.: Stratospheric $BrONO_2$ observed by MIPAS, Atmos. Chem. Phys., 9, 1735–1746, 2009.

Höpfner, M., Glatthor, N., Grabowski, U., Kellmann, S., Kiefer, M., Linden, A., Orphal, J., Stiller, G., von Clarmann, T., Funke, B., and Boone, C. D.: Sulfur dioxide (SO_2) as observed by MIPAS/Envisat: temporal development and spatial distribution at 15–45 km altitude, Atmos. Chem. Phys., 13, 10 405–10 423, doi:10.5194/acp-13-10405-2013, http://www.atmos-chem-phys.net/13/10405/2013/, 2013.

Kiefer, M., von Clarmann, T., Grabowski, U., De Laurentis, M., Mantovani, R., Milz, M., and Ridolfi, M.: Characterization of MIPAS elevation pointing, Atmos. Chem. Phys., 7, 1615–1628, 2007.

Kirkby, J., Curtius, J., Almeida, J., Dunne, E., Duplissy, J., Ehrhart, S., Franchin, A., Gagné, S., Ickes, L., Kürten, A., Kupc, A., Metzger, A., Riccobono, F., Rondo, L., Schobesberger, S., Tsagkogeorgas, G., Wimmer, D., Amorim, A., Bianchi, F., Breitenlechner, M., David, A., Dommen, J., Downard, A., Ehn, M., Flagan, R. C., Haider, S., Hansel, A., Hauser, D., Jud, W., Junninen, H., Kreissl, F., Kvashin, A., Laaksonen, A., Lehtipalo, K., Lima, J., Lovejoy, E. R., Makhmutov, V., Mathot, S., Mikkilä, J., Minginette, P., Mogo, S., Nieminen, T., Onnela, A., Pereira, P., Petäjä, T., Schnitzhofer, R., Seinfeld, J. H., Sipilä, M., Stozhkov, Y., Stratmann, F., Tomé, A., Vanhanen, J., Viisanen, Y., Vrtala, A., Wagner, P. E., Walther, H., Weingartner, E., Wex, H., Winkler, P. M., Carslaw, K. S., Worsnop, D. R., Baltensperger, U., and Kulmala, M.: Role of sulphuric acid, ammonia and galactic cosmic rays in atmospheric aerosol nucleation, Nature, 476, 429–433, doi:10.1038/nature10343, 2011.

Kleinert, A., Aubertin, G., Perron, G., Birk, M., Wagner, G., Hase, F., Nett, H., and Poulin, R.: MIPAS Level 1B algorithms overview: operational processing and characterization, Atmos. Chem. Phys., 7, 1395–1406, doi:10.5194/acp-7-1395-2007, http://www.atmos-chem-phys.net/7/1395/2007/, 2007.

Kürten, A., Münch, S., Rondo, L., Bianchi, F., Duplissy, J., Jokinen, T., Junninen, H., Sarnela, N., Schobesberger, S., Simon, M., Sipilä, M., Almeida, J., Amorim, A., Dommen, J., Donahue, N. M., Dunne, E. M., Flagan, R. C., Franchin, A., Kirkby, J., Kupc, A., Makhmutov, V., Petäjä, T., Praplan, A. P., Riccobono, F., Steiner, G., Tomé, A., Tsagkogeorgas, G., Wagner, P. E., Wimmer, D., Baltensperger, U., Kulmala, M., Worsnop, D. R., and Curtius, J.: Thermodynamics of the formation of sulfuric acid dimers in the binary (H_2SO_4–H_2O) and ternary (H_2SO_4–H_2O–NH_3) system, Atmos. Chem. Phys., 15, 10 701–10 721, doi:10.5194/acp-15-10701-2015, http://www.atmos-chem-phys.net/15/10701/2015/, 2015.

Leen, J. B., Yu, X.-Y., Gupta, M., Baer, D. S., Hubbe, J. M., Kluzek, C. D., Tomlinson, J. M., and Mike R. Hubbell, I.: Fast In Situ Airborne Measurement of Ammonia Using a Mid-Infrared Off-Axis ICOS Spec-

trometer, Environmental Science & Technology, 47, 10 446–10 453, doi:10.1021/es401134u, http://dx.doi.org/10.1021/es401134u, pMID: 23869496, 2013.

Liao, H. and Seinfeld, J. H.: Global impacts of gas-phase chemistry-aerosol interactions on direct radiative forcing by anthropogenic aerosols and ozone, J. Geophys. Res., 110, n/a–n/a, doi:10.1029/2005JD005907, http://dx.doi.org/10.1029/2005JD005907, d18208, 2005.

Martin, S. T., Hung, H.-M., Park, R. J., Jacob, D. J., Spurr, R. J. D., Chance, K. V., and Chin, M.: Effects of the physical state of tropospheric ammonium-sulfate-nitrate particles on global aerosol direct radiative forcing, Atmos. Chem. Phys., 4, 183–214, doi:10.5194/acp-4-183-2004, http://www.atmos-chem-phys.net/4/183/2004/, 2004.

Metzger, S., Dentener, F., Krol, M., Jeuken, A., and Lelieveld, J.: Gas/aerosol partitioning 2. Global modeling results, J. Geophys. Res., 107, ACH 17–1–ACH 17–23, doi:10.1029/2001JD001103, http://dx.doi.org/10.1029/2001JD001103, 2002.

Nowak, J. B., Neuman, J. A., Bahreini, R., Brock, C. A., Middlebrook, A. M., Wollny, A. G., Holloway, J. S., Peischl, J., Ryerson, T. B., and Fehsenfeld, F. C.: Airborne observations of ammonia and ammonium nitrate formation over Houston, Texas, J. Geophys. Res., 115, n/a–n/a, doi:10.1029/2010JD014195, http://dx.doi.org/10.1029/2010JD014195, d22304, 2010.

Oelhaf, H., Leupolt, A., and Fischer, H.: Discrepancies between balloon-borne IR atmospheric spectra and corresponding synthetic spectra calculated line by line around 825 cm^{-1}, Appl. Opt., 22, 647–649, 1983.

Ortega, I. K., Kurtén, T., Vehkamäki, H., and Kulmala, M.: The role of ammonia in sulfuric acid ion induced nucleation, Atmos. Chem. Phys., 8, 2859–2867, doi:10.5194/acp-8-2859-2008, http://www.atmos-chem-phys.net/8/2859/2008/, 2008.

Paulot, F., Jacob, D. J., Pinder, R. W., Bash, J. O., Travis, K., and Henze, D. K.: Ammonia emissions in the United States, European Union, and China derived by high-resolution inversion of ammonium wet deposition data: Interpretation with a new agricultural emissions inventory (MASAGE_NH3), J. Geophys. Res., 119, 4343–4364, doi:10.1002/2013JD021130, http://dx.doi.org/10.1002/2013JD021130, 2014.

Paulot, F., Jacob, D. J., Johnson, M. T., Bell, T. G., Baker, A. R., Keene, W. C., Lima, I. D., Doney, S. C., and Stock, C. A.: Global oceanic emission of ammonia: Constraints from seawater and atmospheric observations, Global Biogeochem. Cycles, 29, 1165–1178, doi:10.1002/2015GB005106, http://dx.doi.org/10.1002/2015GB005106, 2015GB005106, 2015.

Paulot, F., Ginoux, P., Cooke, W. F., Donner, L. J., Fan, S., Lin, M.-Y., Mao, J., Naik, V., and Horowitz, L. W.: Sensitivity of nitrate aerosols to ammonia emissions and to nitrate chemistry: implications for present and future nitrate optical depth, Atmos. Chem. Phys., 16, 1459–1477, doi:10.5194/acp-16-1459-2016, http://www.atmos-chem-phys.net/16/1459/2016/, 2016.

Ploeger, F., Gottschling, C., Griessbach, S., Grooß, J.-U., Guenther, G., Konopka, P., Müller, R., Riese, M., Stroh, F., Tao, M., Ungermann, J., Vogel, B., and von Hobe, M.: A potential vorticity-based determination of the transport barrier in the Asian summer monsoon anticyclone, Atmospheric Chemistry and Physics, 15, 13 145–13 159, doi:10.5194/acp-15-13145-2015, http://www.atmos-chem-phys.net/15/13145/2015/, 2015.

Prenni, A. J., Wise, M. E., Brooks, S. D., and Tolbert, M. A.: Ice nucleation in sulfuric acid and ammonium sulfate particles, Journal of Geophysical Research: Atmospheres, 106, 3037–3044, doi:10.1029/2000JD900454, http://dx.doi.org/10.1029/2000JD900454, 2001.

Atmos. Chem. Phys. Discuss., doi:10.5194/acp-2016-392, 2016
Manuscript under review for journal Atmos. Chem. Phys.
Published: 3 June 2016

Atmospheric Chemistry and Physics Discussions

Rodgers, C. D.: Inverse Methods for Atmospheric Sounding: Theory and Practice, vol. 2 of Series on Atmospheric, Oceanic and Planetary Physics, World Scientific, 2000.

Rothman, L., Gordon, I., Babikov, Y., Barbe, A., Benner, D. C., Bernath, P., Birk, M., Bizzocchi, L., Boudon, V., Brown, L., Campargue, A., Chance, K., Cohen, E., Coudert, L., Devi, V., Drouin, B., Fayt, A., Flaud, J.-M., Gamache, R., Harrison, J., Hartmann, J.-M., Hill, C., Hodges, J., Jacquemart, D., Jolly, A., Lamouroux, J., Roy, R. L., Li, G., Long, D., Lyulin, O., Mackie, C., Massie, S., Mikhailenko, S., Müller, H., Naumenko, O., Nikitin, A., Orphal, J., Perevalov, V., Perrin, A., Polovtseva, E., Richard, C., Smith, M., Starikova, E., Sung, K., Tashkun, S., Tennyson, J., Toon, G., Tyuterev, V., and Wagner, G.: The {HITRAN2012} molecular spectroscopic database, J. Quant. Spectrosc. Radiat. Transfer, 130, 4 – 50, doi:http://dx.doi.org/10.1016/j.jqsrt.2013.07.002, http://www.sciencedirect.com/science/article/pii/S0022407313002859, {HITRAN2012} special issue, 2013.

Schobesberger, S., Junninen, H., Bianchi, F., Lönn, G., Ehn, M., Lehtipalo, K., Dommen, J., Ehrhart, S., Ortega, I. K., Franchin, A., Nieminen, T., Riccobono, F., Hutterli, M., Duplissy, J., Almeida, J., Amorim, A., Breitenlechner, M., Downard, A. J., Dunne, E. M., Flagan, R. C., Kajos, M., Keskinen, H., Kirkby, J., Kupc, A., Kürten, A., Kurtén, T., Laaksonen, A., Mathot, S., Onnela, A., Praplan, A. P., Rondo, L., Santos, F. D., Schallhart, S., Schnitzhofer, R., Sipilä, M., Tomé, A., Tsagkogeorgas, G., Vehkamäki, H., Wimmer, D., Baltensperger, U., Carslaw, K. S., Curtius, J., Hansel, A., Petäjä, T., Kulmala, M., Donahue, N. M., and Worsnop, D. R.: Molecular understanding of atmospheric particle formation from sulfuric acid and large oxidized organic molecules, PNAS, 110, 17 223–17 228, doi:10.1073/pnas.1306973110, http://www.pnas.org/content/110/43/17223.abstract, 2013.

Shephard, M. W. and Cady-Pereira, K. E.: Cross-track Infrared Sounder (CrIS) satellite observations of tropospheric ammonia, Atmos. Meas. Techn., 8, 1323–1336, doi:10.5194/amt-8-1323-2015, http://www.atmos-meas-tech.net/8/1323/2015/, 2015.

Shephard, M. W., Cady-Pereira, K. E., Luo, M., Henze, D. K., Pinder, R. W., Walker, J. T., Rinsland, C. P., Bash, J. O., Zhu, L., Payne, V. H., and Clarisse, L.: TES ammonia retrieval strategy and global observations of the spatial and seasonal variability of ammonia, Atmos. Chem. Phys., 11, 10 743–10 763, doi:10.5194/acp-11-10743-2011, http://www.atmos-chem-phys.net/11/10743/2011/, 2011.

Shindell, D. T., Lamarque, J.-F., Schulz, M., Flanner, M., Jiao, C., Chin, M., Young, P. J., Lee, Y. H., Rotstayn, L., Mahowald, N., Milly, G., Faluvegi, G., Balkanski, Y., Collins, W. J., Conley, A. J., Dalsoren, S., Easter, R., Ghan, S., Horowitz, L., Liu, X., Myhre, G., Nagashima, T., Naik, V., Rumbold, S. T., Skeie, R., Sudo, K., Szopa, S., Takemura, T., Voulgarakis, A., Yoon, J.-H., and Lo, F.: Radiative forcing in the ACCMIP historical and future climate simulations, Atmos. Chem. Phys., 13, 2939–2974, doi:10.5194/acp-13-2939-2013, http://www.atmos-chem-phys.net/13/2939/2013/, 2013.

Spang, R., Remedios, J. J., and Barkley, M. P.: Colour indices for the detection and differentiation of cloud types in infra-red limb emission spectra, Adv. Space Res., 33, 1041–1047, 2004.

Steck, T.: Methods for determining regularization for atmospheric retrieval problems, Appl. Opt., 41, 1788–1797, 2002.

Sutton, M. A., Reis, S., Riddick, S. N., Dragosits, U., Nemitz, E., Theobald, M. R., Tang, Y. S., Braban, C. F., Vieno, M., Dore, A. J., Mitchell, R. F., Wanless, S., Daunt, F., Fowler, D., Blackall, T. D., Milford, C., Flechard, C. R., Loubet, B., Massad, R., Cellier, P., Personne, E., Coheur, P. F., Clarisse, L., Van Damme,

Atmos. Chem. Phys. Discuss., doi:10.5194/acp-2016-392, 2016
Manuscript under review for journal Atmos. Chem. Phys.
Published: 3 June 2016

M., Ngadi, Y., Clerbaux, C., Skjøth, C. A., Geels, C., Hertel, O., Wichink Kruit, R. J., Pinder, R. W., Bash, J. O., Walker, J. T., Simpson, D., Horváth, L., Misselbrook, T. H., Bleeker, A., Dentener, F., and de Vries, W.: Towards a climate-dependent paradigm of ammonia emission and deposition, Philosophical Transactions of the Royal Society of London B: Biological Sciences, 368, doi:10.1098/rstb.2013.0166, http://rstb.royalsocietypublishing.org/content/368/1621/20130166, 2013.

Tabazadeh, A. and Toon, O. B.: The role of ammoniated aerosols in cirrus cloud nucleation, Geophys. Res. Lett., 25, 1379–1382, doi:10.1029/97GL03585, http://dx.doi.org/10.1029/97GL03585, 1998.

Tikhonov, A.: On the solution of incorrectly stated problems and method of regularization, Dokl. Akad. Nauk. SSSR, 151, 501–504, 1963.

Van Damme, M., Clarisse, L., Heald, C. L., Hurtmans, D., Ngadi, Y., Clerbaux, C., Dolman, A. J., Erisman, J. W., and Coheur, P. F.: Global distributions, time series and error characterization of atmospheric ammonia (NH_3) from IASI satellite observations, Atmos. Chem. Phys., 14, 2905–2922, doi:10.5194/acp-14-2905-2014, http://www.atmos-chem-phys.net/14/2905/2014/, 2014.

Van Damme, M., Erisman, J. W., Clarisse, L., Dammers, E., Whitburn, S., Clerbaux, C., Dolman, A. J., and Coheur, P.-F.: Worldwide spatiotemporal atmospheric ammonia (NH3) columns variability revealed by satellite, Geophys. Res. Lett., 42, 8660–8668, doi:10.1002/2015GL065496, http://dx.doi.org/10.1002/2015GL065496, 2015GL065496, 2015.

Vernier, J.-P., Thomason, L. W., and Kar, J.: CALIPSO detection of an Asian tropopause aerosol layer, Geophys. Res. Lett., 38, doi:10.1029/2010GL046614, http://dx.doi.org/10.1029/2010GL046614, 2011.

von Bobrutzki, K., Braban, C. F., Famulari, D., Jones, S. K., Blackall, T., Smith, T. E. L., Blom, M., Coe, H., Gallagher, M., Ghalaieny, M., McGillen, M. R., Percival, C. J., Whitehead, J. D., Ellis, R., Murphy, J., Mohacsi, A., Pogany, A., Junninen, H., Rantanen, S., Sutton, M. A., and Nemitz, E.: Field inter-comparison of eleven atmospheric ammonia measurement techniques, Atmos. Meas. Techn., 3, 91–112, doi:10.5194/amt-3-91-2010, http://www.atmos-meas-tech.net/3/91/2010/, 2010.

von Clarmann, T., Glatthor, N., Grabowski, U., Höpfner, M., Kellmann, S., Kiefer, M., Linden, A., Mengistu Tsidu, G., Milz, M., Steck, T., Stiller, G. P., Wang, D. Y., Fischer, H., Funke, B., Gil-López, S., and López-Puertas, M.: Retrieval of temperature and tangent altitude pointing from limb emission spectra recorded from space by the Michelson Interferometer for Passive Atmospheric Sounding (MIPAS), J. Geophys. Res., 108, 4736, doi:10.1029/2003JD003602, 2003.

von Clarmann, T., Höpfner, M., Kellmann, S., Linden, A., Chauhan, S., Funke, B., Grabowski, U., Glatthor, N., Kiefer, M., Schieferdecker, T., Stiller, G. P., and Versick, S.: Retrieval of temperature, H_2O, O_3, HNO_3, CH_4, N_2O, $ClONO_2$ and ClO from MIPAS reduced resolution nominal mode limb emission measurements, Atmos. Meas. Techn., 2, 159–175, 2009.

Vuuren, D. P., Edmonds, J., Kainuma, M., Riahi, K., Thomson, A., Hibbard, K., Hurtt, G. C., Kram, T., Krey, V., Lamarque, J.-F., Masui, T., Meinshausen, M., Nakicenovic, N., Smith, S. J., and Rose, S. K.: The representative concentration pathways: an overview, Climatic Change, 109, 5–31, doi:10.1007/s10584-011-0148-z, http://dx.doi.org/10.1007/s10584-011-0148-z, 2011.

Wang, J., Hoffmann, A. A., Park, R. J., Jacob, D. J., and Martin, S. T.: Global distribution of solid and aqueous sulfate aerosols: Effect of the hysteresis of particle phase transitions, J. Geophys. Res., 113, n/a–n/a, doi:10.1029/2007JD009367, http://dx.doi.org/10.1029/2007JD009367, d11206, 2008.

Atmos. Chem. Phys. Discuss., doi:10.5194/acp-2016-392, 2016
Manuscript under review for journal Atmos. Chem. Phys.
Published: 3 June 2016

Atmospheric Chemistry and Physics Discussions

Warner, J. X., Wei, Z., Strow, L. L., Dickerson, R. R., and Nowak, J. B.: The global tropospheric ammonia distribution as seen in the 13-year AIRS measurement record, Atmospheric Chemistry and Physics, 16, 5467–5479, doi:10.5194/acp-16-5467-2016, http://www.atmos-chem-phys.net/16/5467/2016/, 2016.

Wise, M. E., Garland, R. M., and Tolbert, M. A.: Ice nucleation in internally mixed ammonium sulfate/dicarboxylic acid particles, Journal of Geophysical Research: Atmospheres, 109, n/a–n/a, doi:10.1029/2003JD004313, http://dx.doi.org/10.1029/2003JD004313, d19203, 2004.

Xu, L. and Penner, J. E.: Global simulations of nitrate and ammonium aerosols and their radiative effects, Atmos. Chem. Phys., 12, 9479–9504, doi:10.5194/acp-12-9479-2012, http://www.atmos-chem-phys.net/12/9479/2012/, 2012.

Ziereis, H. and Arnold, F.: Gaseous ammonia and ammonium ions in the free troposphere, Nature, 321, 503–505, doi:10.1038/321503a0, 1986.

Atmos. Chem. Phys. Discuss., doi:10.5194/acp-2016-392, 2016
Manuscript under review for journal Atmos. Chem. Phys.
Published: 3 June 2016

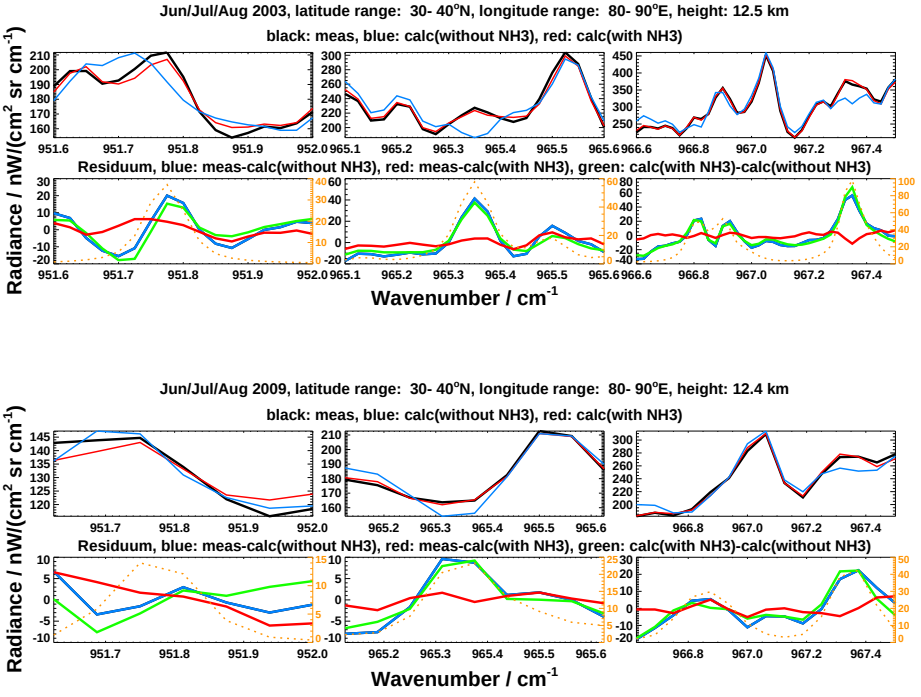

Figure 1. Spectral identification of NH_3 in MIPAS observations within the three spectral windows used for the retrieval (columns). The top two rows belong to the first observational period with higher spectral resolution. Rows 3 and 4 refer to the second period with lower spectral resolution. Rows 1 and 3 contain measured (black) and best fit spectra (blue: without, red: with NH_3). Row 2 and 4 show the spectral residuals without consideration of NH_3 (blue) and with NH_3 (red). Green curves in the second and fourth row represent the spectral features of NH_3 (calculation with NH_3 minus calculation without NH_3). To guide the eye, the orange dashed lines in rows 2 and 4 are simulated pure NH_3 spectra.

Atmos. Chem. Phys. Discuss., doi:10.5194/acp-2016-392, 2016
Manuscript under review for journal Atmos. Chem. Phys.
Published: 3 June 2016

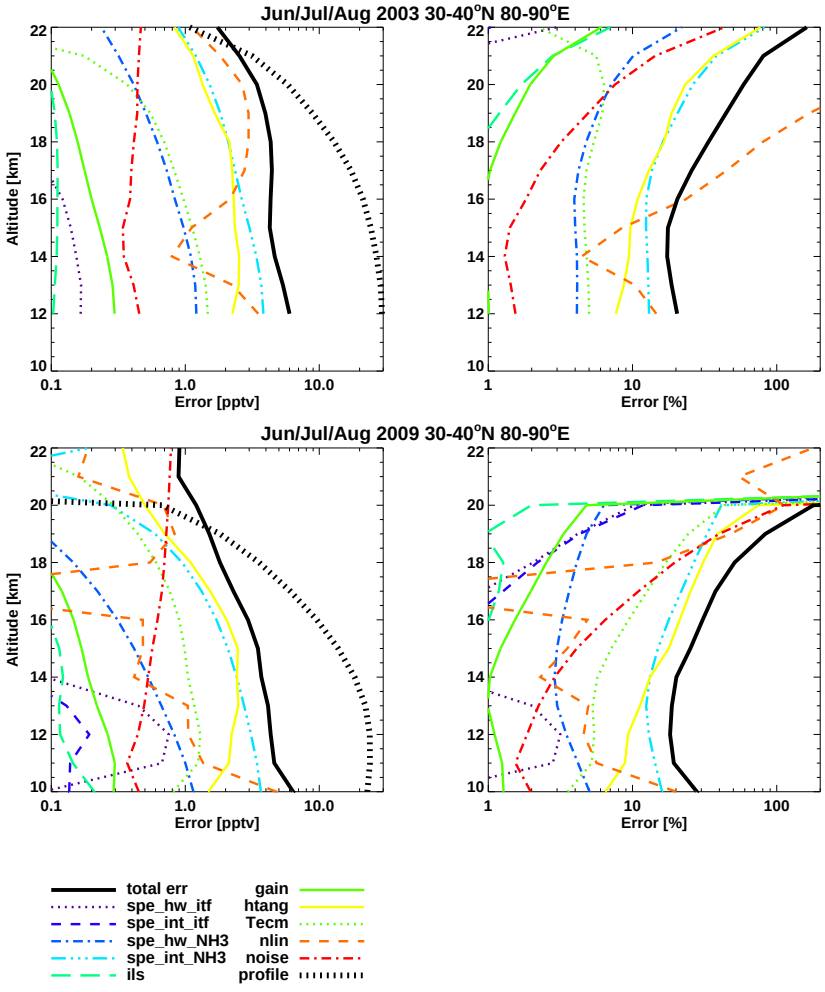

Figure 2. Estimated error profiles for two examples: one from measurement period 1 (June/July/August 2003, 30–40°N, 80–90°E) and one from period 2 (June/July/August 2009, 30–40°N, 80–90°E). The retrieved NH_3 vmr profiles are shown as bold black dotted lines ("profile"). Abbreviations of the error sources are resolved in Tab. 1.

Atmos. Chem. Phys. Discuss., doi:10.5194/acp-2016-392, 2016
Manuscript under review for journal Atmos. Chem. Phys.
Published: 3 June 2016

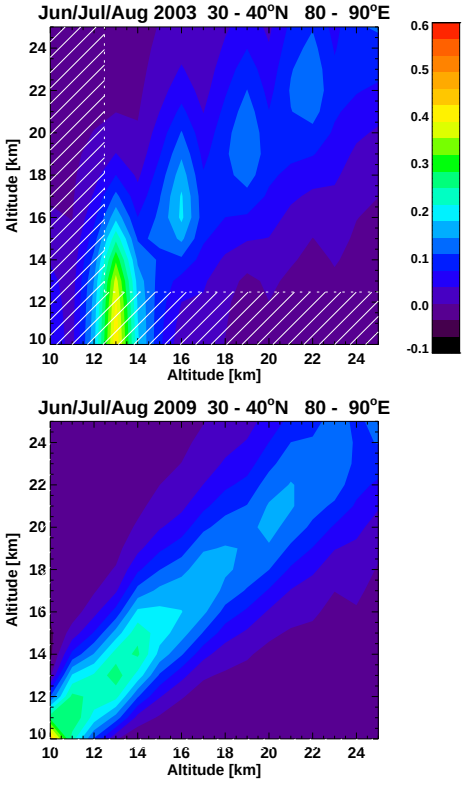

Figure 3. Averaging kernels of the MIPAS NH_3 retrieval during the first (top) and second (bottom) MIPAS measurement period. The number of degrees-of-freedom up to 25 km is 2.1 (top) and 3.5 (bottom). Hatched areas indicate altitudes below the lowest tangent height where no measurement information is available.

Atmos. Chem. Phys. Discuss., doi:10.5194/acp-2016-392, 2016
Manuscript under review for journal Atmos. Chem. Phys.
Published: 3 June 2016

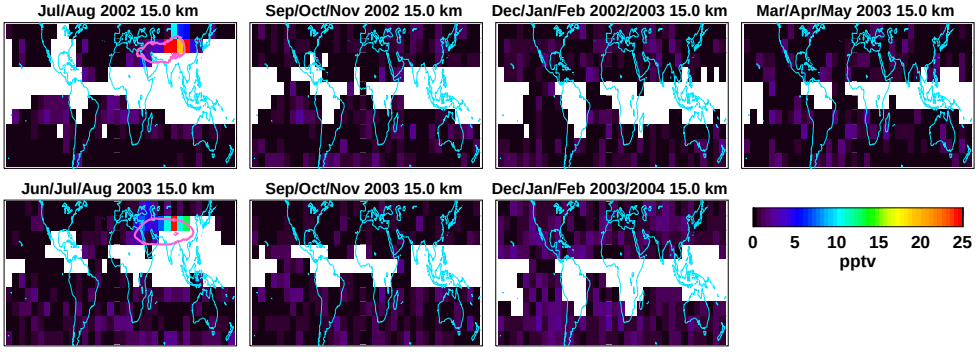

Figure 4. Distributions of NH_3 volume mixing ratios at 15 km altitude between 50°N and 50°S retrieved from MIPAS seasonal mean spectra during the first measurement period. Pixels where not enough spectra for averaging were available are left white. To guide the eye, the pink lines denote the approximate position of the Asian Monsoon Anticyclone. It is the 2×10^{-6} $\mathrm{Km^2kg^{-1}s^{-1}}$ contour of the mean potential vorticity for July/August in 2002 and June/July/August in 2003 at the potential temperature level of 370 K from the ECMWF ERA interim reanalysis (e.g. Ploeger et al., 2015, and references therein).

Atmos. Chem. Phys. Discuss., doi:10.5194/acp-2016-392, 2016
Manuscript under review for journal Atmos. Chem. Phys.
Published: 3 June 2016

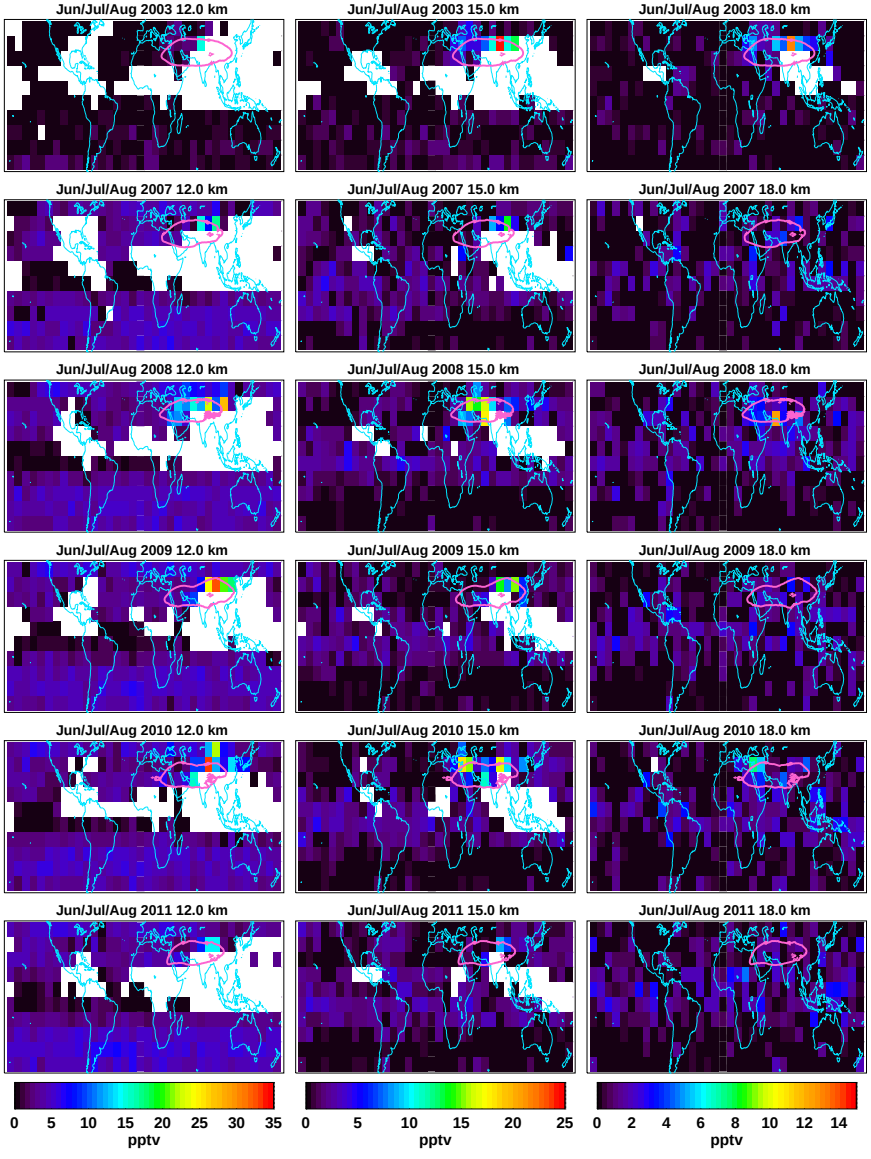

Figure 5. Distributions of NH_3 volume mixing ratios at 12 km, 15 km and 18 km altitude between 50°N and 50°S retrieved from MIPAS seasonal mean spectra for several years during the Asian monsoon period. Pixels where not enough spectra for averaging were available are left white. Pink contour lines denote the mean position of the Asian Monsoon Anticyclone for June/July/August as described in the caption of Fig. 4.

Atmos. Chem. Phys. Discuss., doi:10.5194/acp-2016-392, 2016
Manuscript under review for journal Atmos. Chem. Phys.
Published: 3 June 2016

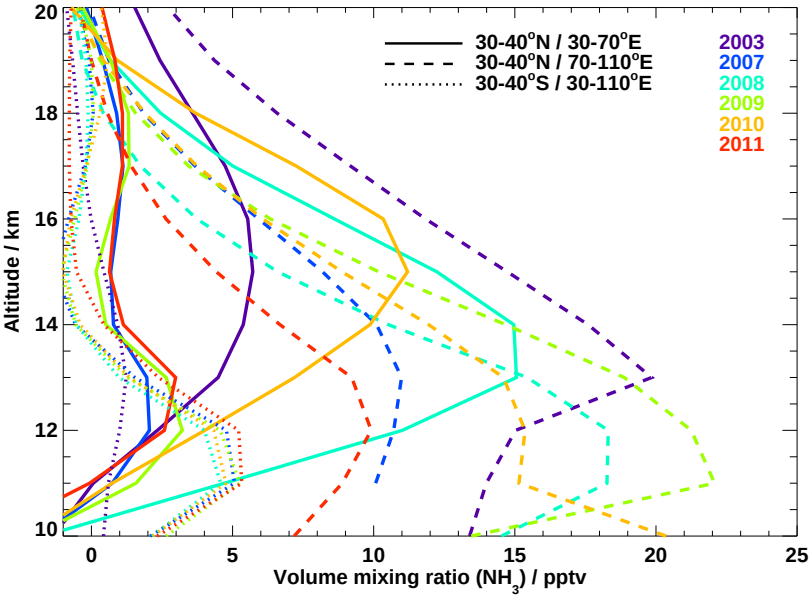

Figure 6. Mean profiles of NH_3 from MIPAS within the geographical range noted in the figure legend during June/July/August of each year. Solid: westerly part, dashed: easterly part of the Asian monsoon, dotted: reference profiles outside the monsoon in the southern hemisphere.

Atmos. Chem. Phys. Discuss., doi:10.5194/acp-2016-392, 2016
Manuscript under review for journal Atmos. Chem. Phys.
Published: 3 June 2016

Atmospheric Chemistry and Physics Discussions

Table 1. Assumptions on uncertainties used for the error assessment in Fig. 2.

Error source	Assumed uncertainty	Abbreviation
Spectral noise after apodization[1]	period 1: 2.2 (1.5–3.1) $\mathrm{nW/(cm^2 sr\,cm^{-1})}$	noise
	period 2: 1.3 (0.8–1.8) $\mathrm{nW/(cm^2 sr\,cm^{-1})}$	
Instrument line shape[2]	3%	ils
Instrument gain calibration[3]	1%	gain
Tangent altitude[4]	300 m	htang
Temperature[5]	2 K below/5 K above 35 km	Tecm
Retrieval from averaged spectra[6]		nlin
Air-broadened half-width of NH_3 lines[7]	10%	spe_hw_NH_3
Intensity of NH_3 lines[7]	15%	spe_int_NH_3
Air-broadened half-width of interfering gas lines[7]	15%	spe_hw_itf
Intensity of interfering gas lines[7]	5%	spe_int_itf

[1] ESA 11b dataset, depending on number of co-added spectra; [2] F. Hase, pers. comm., Höpfner et al. (2007); [3] Kleinert et al. (2007); [4] von Clarmann et al. (2003); von Clarmann et al. (2009); Kiefer et al. (2007); [5] ECMWF uncertainty Höpfner et al. (2013); [6] Höpfner et al. (2009); Höpfner et al. (2013); [7] HITRAN 2012 spectral line errors Rothman et al. (2013)